ANALYSIS OF URINARY STONES COLLECTED FROM SOME PATIENTS WITH X-RAY DIFFRACTION, FOURIER TRANSFORM INFRARED SPECTROSCOPY, AND SCANNING ELECTRON MICROSCOPY

M. Serkan Yalçın [1*], Mesut Tek [2]

[1] Mersin University, Technical Science Vocational School, Department of Chemical and Chemical Processing Technologies, 33343, Mersin, Turkey; e-mail: serkanyalcin@mersin.edu.tr
[2] Mersin University, Faculty of Medicine, Department of Urology, 33343, Mersin, Turkey

This study aims to determine the urinary stones' chemical compositions, morphologies and crystal size by using X-ray diffraction, scanning electron microscopy with energy dispersive X-ray, and Fourier transform infrared spectroscopy. This study has been conducted with 30 urinary stones from the 30 patients who were treated at the Department of Urology in Mersin University Hospital (Mersin, Turkey). With respect to the detected phase compositions, results were classified into four chemical groups: oxalates (43.3%), phosphates (13.3%), urates (6.7%), and mixed stone (36.7%).

Keywords: *urinary stones, urolithiasis, X-ray diffraction, Fourier transform infrared spectroscopy, scanning electron microscopy with energy dispersive X-ray.*

АНАЛИЗ СОСТАВА МОЧЕВЫХ КАМНЕЙ МЕТОДАМИ РЕНТГЕНОВСКОЙ ДИФРАКЦИИ, ИНФРАКРАСНОЙ СПЕКТРОСКОПИИ С ФУРЬЕ-ПРЕОБРАЗОВАНИЕМ И СКАНИРУЮЩЕЙ ЭЛЕКТРОННОЙ МИКРОСКОПИИ

M. Serkan Yalçın [1*], M. Tek [2]

УДК 543.42.062:616.62-003.7

[1] Техническое профессиональное училище Университета Мерсин, 33343, Мерсин, Турция; e-mail: serkanyalcin@mersin.edu.tr
[2] Университет Мерсин, 33343, Мерсин, Турция

(Поступила 22 ноября 2017)

С помощью методов рентгеновской дифракции, сканирующей электронной микроскопии с энергодисперсионной рентгеновской спектрометрией и инфракрасной спектроскопии с Фурье-преобразованием определены химический состав, морфология и размеры кристаллов мочевых камней. Исследование проводилось на 30 мочевых камнях, взятых у 30 пациентов, находившихся на лечении в урологическом отделении больницы Университета Мерсин (Турция). Показано, что в составе камней присутствуют четыре химические группы: оксалаты (43.3 %), фосфаты (13.3 %), ураты (6.7 %) и смешанный камень (36.7 %).

Ключевые слова: *мочевые камни, мочекаменная болезнь, рентгеновская дифракция, инфракрасная спектроскопия с преобразованием Фурье, сканирующая электронная микроскопия с энергодисперсионной рентгеновской спектрометрией.*

Introduction. Urolithiasis, a widespread urinary system disease, affects up to 10–20% of the general population. Its treatment process takes a long time and the recurrence rate reaches up to 50% [1–3]. This disease results from stone formation in the urinary system, called urinary stones. Urolithiasis disease is one of the most common diseases seen in urology practice. In terms of frequency, it is three times more common among men aged between 20–50 than among women. Although it is less frequently observed among the black race, it is never seen at all among Eskimos whose diet consist mainly of fish. This disease is frequently seen in hot climates and in communities largely consuming protein and carbohydrates. In childhood, it

appears equally in boys and girls, and it usually tends to repeat approximately until the age of 18 [4]. However, the mechanism of the stone formation has not been understood clearly, yet. The chemical analysis of the formed stone and the clarification of its structure is very important for correct diagnosis and treatment in terms of understanding its nature and etiology [5–8]. The structure and composition of these stones are generally complicated because they are influenced by many factors such as the environment, the climate conditions in which the individual lives, diet, age, gender, fluid intake, quality of drinking water, and metabolism of the individual [9–12]. The components of the stones may consist of a mixture of crystal and organic material at certain ratios [13]. Examples of the most common samples are calcium oxalate monohydrate known as whewellite ($CaC_2O_4 \cdot H_2O$), calcium oxalate dihydrate known as weddellite ($CaC_2O_4 \cdot 2H_2O$), calcium phosphate known as apatite $\{Ca_{10}(PO_4,CO_3)_6(OH,CO_3)\}$, calcium hydrogen phosphate dihydrate known as brushite ($CaHPO_4 \cdot 2H_2O$), magnesium ammonium phosphate hexahydrate ($MgNH_4\ PO_4 \cdot 6H_2O$) also known as sitruvite, and uric acid ($C_5H_4N_4O_3$). There are 82 known components in the urinary system stones, but only seven of them exist in more than 1% of stones [14]. Although 75% of the stones of the urinary system are calcium oxalate based, some are present in mixed form [15, 16].

The most commonly methods used in the analysis of urinary system stones are polarized microscopy, chemical methods in the form of analysis kit, and XRD and FT-IR techniques, which are more modern techniques. Accurate results can be obtained with a polarized microscope, but it requires expertise, and the accuracy of the results depends the individual. The results obtained with chemical methods are limited and require accurate interpretation [17]. XRD and FT-IR are the most powerful techniques that come to the forefront in this field due to the disadvantages of polarized microscopy and chemical methods. FT-IR is a fast and easy-to-apply technique, although it remains insufficient for quantitative analysis of stones with mixed conformation containing multicomponent phases [18, 19]. The XRD can clarify the composition of the urinary system stones in a fast, reliable and highly accurate way without exposing them to any corruptive effects and can quantitatively give the chemical composition of the stone-forming phases [20–22]. In addition, Corns [23] emphasizes that X-ray diffraction analysis can give information which any other method cannot provide, such as the separation of phases of $Ca(COO)_2 \cdot H_2O$ and $Ca(COO)_2$.

This study investigated the chemical composition and morphological characteristics of urinary system stones belonging to urolithiasis patients who applied to the Urology Department of Mersin University Medical Faculty Hospital by using XRD, FT-IR, SEM and EDX.

Experimental. Thirty urinary stones (Fig. 1) were obtained from 30 patients who were treated for urolithiasis disease in the Department of Urology, Mersin University Hospital, Mersin, Turkey. Informed consent was taken from all patients. The study was approved by the Mersin University Clinical Research Ethics Committee (2016/139). Prior to analysis, stones were carefully washed by using deionized water in order to eliminate blood clots and were air-dried afterwards. The homogeneity and representability of the samples were achieved by crushing the stones down to 3–5 mm size followed by quartering. After that, the stones were ground manually in a mortar to a powder with a grain size of about 5–10 μm which subsequently was filled into a low-background quartz sample holder. The XRD analysis of the stones was carried out using a SmartLab Rigaku X-ray diffractometer which operates at 30 kV/40 mA. The use of Ni-filtered CuK_α radiation (k = 1.5405 Å) with a step size of 0.02° at a 2θ range of 7–70° in a continuous scanning mode at a scanning speed of 5°/min was another analysis condition. Phase identification, quantitative phase analysis, and crystallite size calculation were determined by using PDXL2 software. In PDXL2, phase quantification was applied via the normalized reference intensity ratio (RIR) method, and the content of each crystalline phase was calculated as follows:

$$C_i = 100(I_i/k_i)/\sum_{i=1}^{n}\left(l_i / k_i\right), \tag{1}$$

where C_i is the content of ith phase, I_i is the integral intensity of ith phase, and k_i is the corundum coefficient (RIR) for ith phase. The k_i values for analyzed phases are stored in the PDF2 database.

The value of crystallite size was calculated using the Scherrer equation:

$$d = K\lambda/\beta\cos\theta, \tag{2}$$

where d is the average crystallite size, λ is the wavelength of the X-ray radiation, β is full width at half maximum (FWHM) (β is expressed in radians), θ is the Bragg angle for the most intense peak, and K is the Scherrer constant.

Fig. 1. Photographs of some studied urinary stones: A (oxalates), B (phosphates), C (urates), and D (mixed stone).

The mid region (4000–400 cm^{-1}) room temperature FT-IR spectral analysis was carried out with the Perkin Elmer spectrum Frontier using the attenuated total reflectance (ATR) technique. Morphologies of the stones were imagined by the SEM on a Zeiss Supra55 scanning electron microscope. The elemental compositions of the stones were successfully obtained by EDX attached with the SEM.

Results and discussion. *XRD Analysis*. The crystalline phases detected in samples of S1–S30 analyzed by powder XRD method are whewellite, weddellite, struvite, uricide, uric acid dihydrate, brushite, hydroxyapatite, and whitlockite. These crystalline phases were identified using the PDF-2 database (International Center for Diffraction Data 2010). The crystal sizes, chemical compositions and card numbers of these identified crystalline phases are given in Table 1. According to the observed phase compositions, all the studied stones were classified into four chemical groups: oxalates, phosphates, urates and mixtures (Fig. 2). The powder XRD diffraction patterns of these groups are given in Fig. 3. According to this grouping, all analyzed samples included 43.3% oxalates, 13.3% phosphates, 6.7% urates, and 36.7% mixtures. These results are similar to the data reported by Uvarov et al. [20] for Israel, Abboud [24] for North Jordan, Dursun et al. [25] for Turkey, and Trinchieri et al. [26] for Italy.

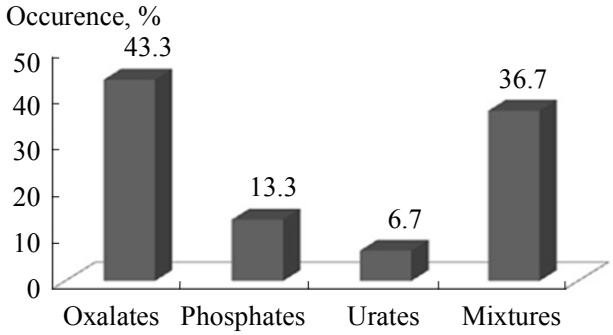

Fig. 2. The occurrence of each allocated chemical group within the whole sampling of the tested kidney stones.

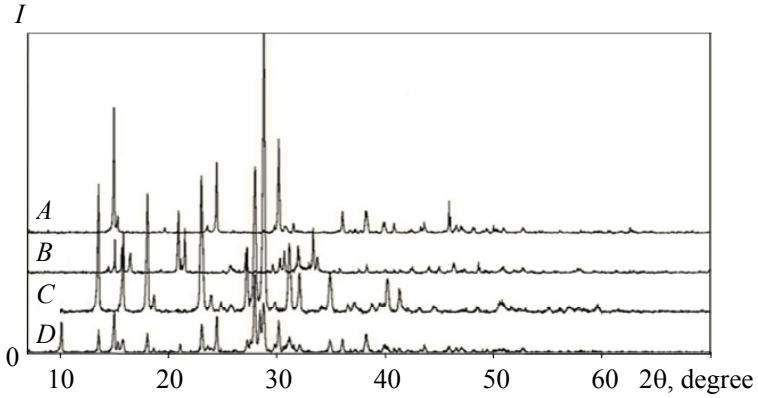

Fig. 3. X-Ray Diffraction patterns of A (oxalates), B (phosphates), C (urates), and D (mixed).

TABLE 1. Calculated Crystal Sizes, Chemical Compositions and Card Numbers of the S1-S30

Sample	*D*, nm	Composition	Formula	DB Card No.
S1	68.6	Struvite	$NH_4MgPO_4 \cdot 6H_2O$	00-015-0762
S2	83.4	Whewellite	$CaC_2O_4 \cdot H_2O$	01-075-1313
S3	177.4	Whewellite (64.0%)	$CaC_2O_4(H_2O)$	01-075-1313
	135.8	Weddellite (36.0%)	$CaC_2O_4(H_2O)_{2.375}$	01-075-1314
S4	42.2	Uricide	$C_5H_4N_4O_3$	00-031-1982
S5	126.5	Whewellite	$CaC_2O_4 \cdot H_2O$	01-075-1313
S6	37.0	Uricide (52.0%)	$C_5H_4N_4O_3$	00-031-1982
	49.4	Whewellite (22.0%)	$CaC_2O_4 \cdot H_2O$	00-020-0231
	47.5	Uric acid dihydrate (26.0%)	$C_5H_4N_4O_3 \cdot 2H_2O$	00-019-1996
S7	38.3	Weddellite	$CaC_2O_4(H_2O)_{2.375}$	01-075-1314
S8	72.3	Whewellite	$CaC_2O_4(H_2O)$	01-075-1313
S9	94.0	Whewellite	$CaC_2O_4(H_2O)$	01-075-1313
S10	61.9	Whewellite	$CaC_2O_4(H_2O)$	01-075-1313
S11	278.1	Whewellite (38.0%)	$CaC_2O_4(H_2O)$	01-075-1313
	55.1	Weddellite (62.0%)	$CaC_2O_4(H_2O)_{2.375}$	01-075-1314
S12	131.0	Struvite	$NH_4MgPO_4 \cdot 6H_2O$	00-015-0762
S13	136.4	Whewellite	$CaC_2O_4(H_2O)$	01-075-1313
S14	138.9	Brushite (56.0%)	$Ca(HPO_4)(H_2O)_2$	01-072-0713
	165.8	Weddellite (44.0%)	$CaC_2O_4(H_2O)_{2.375}$	01-075-1314
S15	181.8	Whewellite	$CaC_2O_4(H_2O)$	01-075-1313
S16	46.6	Uricide (81.0%)	$C_5H_4N_4O_3$	00-031-1982
	55.4	Whewellite (19.0%)	$CaC_2O_4(H_2O)$	01-075-1313
S17	81.7	Uricide (91.9%)	$C_5H_4N_4O_3$	00-031-1982
	47.1	Uric acid dihydrate (8.1%)	$C_5H_4N_4O_3 \cdot 2H_2O$	00-019-1996
S18	4.6	Hydroxyapatite	$Ca_{10}(PO_4,CO_3)_6(OH,CO_3)$	01-075-3729
S19	36.3	Uricide	$C_5H_4N_4O_3$	00-031-1982
S20	106.5	Whewellite (94.3%)	$CaC_2O_4(H_2O)$	01-075-1313
	173.5	Weddellite (5.7%)	$CaC_2O_4(H_2O)_{2.375}$	01-075-1314
S21	46.7	Uricide (64.1%)	$C_5H_4N_4O_3$	00-031-1982
	64.8	Whewellite (35.9%)	$CaC_2O_4(H_2O)$	01-075-1313
S22	111.8	Whewellite (59.0%)	$CaC_2O_4(H_2O)$	01-075-1313
	109.9	Weddellite (41.0%)	$CaC_2O_4(H_2O)_{2.375}$	01-075-1314
S23	94.2	Whewellite	$CaC_2O_4(H_2O)$	01-075-1313
S24	72.6	Whewellite	$CaC_2O_4(H_2O)$	01-075-1313
S25	52.9	Whitlockite	$Ca_9(Mg_{0.62}Fe_{0.35}Mn_{0.02}Al_{0.02})(PO_4)_6(P_{0.94}O_{3.17}(OH))$	01-080-4739
S26	103.7	Whewellite	$CaC_2O_4(H_2O)$	01-075-1313
S27	211.9	Whewellite	$CaC_2O_4(H_2O)$	01-075-1313
S28	98.4	Whewellite	$CaC_2O_4(H_2O)$	01-075-1313
S29	123.5	Whewellite (94.7%)	$CaC_2O_4(H_2O)$	01-075-1313
	74.7	Weddellite (5.3%)	$CaC_2O_4(H_2O)_{2.375}$	01-075-1314
S30	80.0	Struvite (97%)	$NH_4MgPO_4 \cdot 6H_2O$	00-015-0762
	67.0	Weddellite (3.0%)	$CaC_2O_4(H_2O)_{2.375}$	01-075-1314

Detailed analysis of the mixtures samples (i.e., stones, which are composed of a number of crystalline phases belonging to different chemical groups or multiphase samples composed of the phases belonging to the same chemical group) has emphasized that they were composed of different percentage of phase compositions. As shown in Table 1, S3, S6, S11, S14, S16, S17, S20, S21, S22, S29, and S30 were composed of whewellite (64.0%)+weddellite (36.0%), uricide (52.0%)+whewellite (22.0%)+uric acid dihydrate (26.0%), whewellite (38.0%)+weddellite (62.0%), brushite (56.0%)+weddellite (44.0%), uricide (81.0%)+whewellite (19.0%), uricide (91.9%)+uric acid dihydrate (8.1%), whewellite (94.3%)+weddellite (5.7%), uricide (64.1%) + + whewellite (35.9%), whewellite (59.0%)+weddellite (41.0%), whewellite (94.7%)+weddellite (5.3%), and struvite (97%)+weddellite (3.0%), respectively.

The crystal size is a significant parameter and naturally related to the growth conditions of the crystalline phases. Because of this, it affected the chemistry of growth medium and its thermodynamics, which are both defined by the metabolism of the patient. The average crystal sizes of oxalates, phosphates, and urates were found to be 106, 64, and 39 nm, respectively.

Data related to the geographical distribution of diseases are important for medicine and other sciences. These data can be used to examine the geological and environmental factors of some diseases and to eliminate or control the factors which cause some diseases [27]. Since the prevalence of urinary system stones is high in regions with hot climate [28], it is possible to conclude that this disease is directly related to climatic conditions [27, 29]. In addition, the hardness of drinking water is one of the environmental factors that affect the health of the community [27]. Previous studies show that there is a positive and negative directional relationship between water hardness and the prevalence of urinary system stones [30]. Consequently, compatible results were obtained when we compared the results of our powder XRD analysis with the studies conducted in geographical regions in which similar climate and environmental factors prevail [19, 20, 26, 31].

FT-IR Analysis. The FT-IR spectra of the groups of oxalates, phosphates, urates and mixed stones are represented in Fig. 4, and assignments of vibrational bands are given in Table 2. For oxalates the O–H stretching was observed in the region of 3000–3500 cm^{-1}. The peaks at 1618 and 1316 cm^{-1} were due to C=O and C–O stretching, respectively. The bands at 884 and 778 cm^{-1} were attributed to C–C stretching [32]. The appearance of bands at 519 and 508 cm^{-1} are considered to O–C–O in plane bending [33] (Fig. 4A).

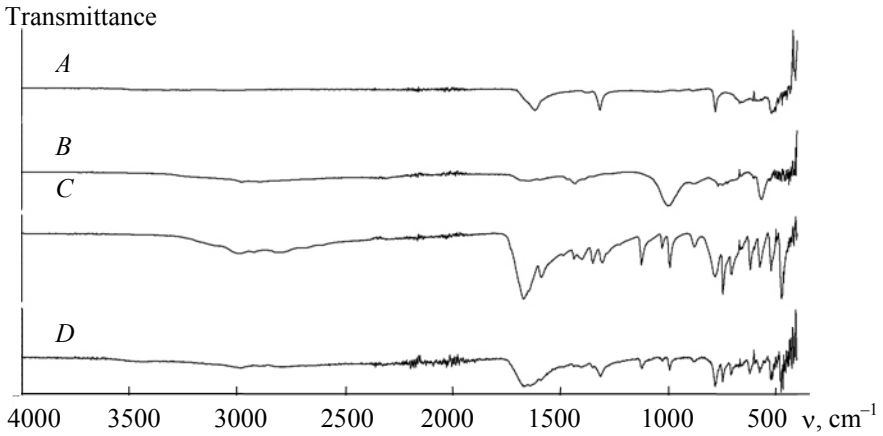

Fig. 4. Fourier transform infrared spectroscopy spectra of the group A (oxalates), B (phosphates), C (urates), and D (mixed stone).

TABLE 2. Fourier Transform Infrared Spectroscopy Spectral Data (cm^{-1}) of the Groups of Oxalates, Phosphates, and Urates

Phases	Wavenumber, cm^{-1}	IR
A (oxalates)	3500–3000	O–H stretching
	1618, 1316	C=O and C–O stretching
	884, 778	C–C stretching
	519, 508	O–C–O in plane bending
B (phosphates)	2900, 1645	Different modes of vibration of water
	1432	Ammonia bands
	1001, 565	Phosphate bands
C (urates)	3600–2600	Heteroaromatic N–H stretching
	1670	C=O stretching
	1590	C=N stretching
	1437, 1405	C=C stretching
	1348, 1308	O–H deformation
	1123, 1026, 991	Ring vibration
	617	Ring breathing mode
	573, 469, 463	Skeletal ring deformation

In the presence of phosphates, the weaker band at 1432 cm^{-1} corresponded to N–H deformation [22] and the strong band at 1001 cm^{-1} is due to the PO_4^{3-} stretching (Fig. 4B). N–H stretching of urates was observed in the range of 3600–2600 cm^{-1}. The bands at 1670 and 1437 cm^{-1} were attributed to C=O stretching and C=C stretching, respectively. The peaks at 1590 and 1123 cm^{-1} corresponded to the conjugated group of amide [11].

SEM and EDX analysis. The surface morphologies and the elemental compositions of the urinary stones were investigated by using the SEM combined with EDX. The SEM micrograph and EDX results of the samples A (oxalates), B (phosphates), C (urates), and D (mixed stone) are shown in Fig. 5. A contains spherulitic crystals of oxalates. B has a rough surface and no obvious shape, C consists of uniform needle shaped crystals [34], and D shows the typical platy crystals of mixed stones.While morphologies of the urinary stones have different shapes, the EDX analysis of each stone confirmed the exact chemical formula derived from XRD.

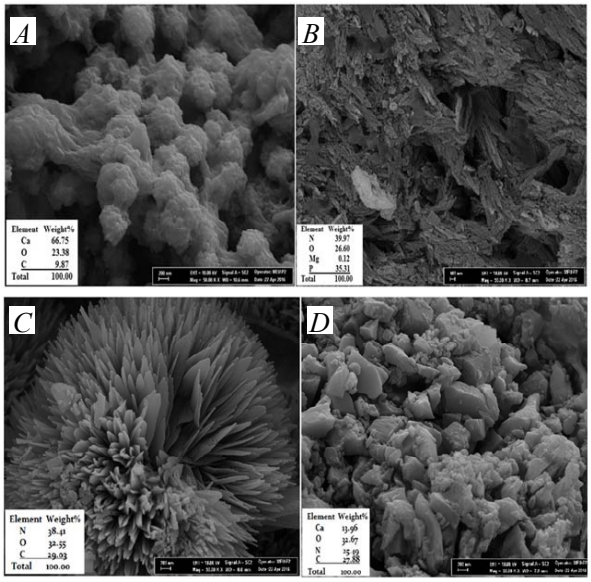

Fig. 5. Scanning electron microscopy micrographs and energy dispersive X-ray results of the group A (oxalates), B (phosphates), C (urates), and D (mixed stone).

Effect of stone type in treatment of urolithiasis. Probably, different mechanisms of stone formation point out different pathologies underlying stone formation and consequently needing different methods for optimal treatment of the underlying disease. Therefore, this situation indicated different paths for optimal treatment of the underlying disease [35]. The treatment of urolithiasis generally consists of three parts: diagnosis, disease management, and follow up of metabolic evaluation and prevention of recurrence [4]. The disease management and the follow-up of urolithiasis usually include pharmacological therapy and surgical approaches if necessary. Depending on the chemical composition of urinary system stones, the treatment is applied with medication, which aims to reduce the recurrence and the size of stones [36, 37]. Depending on the type of the stone, patients may be able to prevent the stone formation by changing the quantity of animal protein, sodium, oxalate, or calcium included in their daily diet [38].

Conclusion. The present study reports the results of a quantitative phase analysis using XRD and vibrational spectra as well as FT-IR on 30 urinary stones collected from Mersin, Turkey. Also the relation between the phase composition and the morphological aspects in the tested urinary stones was studied by using SEM coupled with EDX. The analyzed stones were classified into chemical groups according to their phase compositions. Calcium oxalate was a dominant mineral within all crystalline phases. Whewellite and weddellite were the most common biomineral components in the tested urinary stones. These results show close similarity to the previously published data.

This study reveals that XRD is a powerful, sensitive, reliable, and fast method for the detection of the different kinds of the urinary stone. Our current study may be useful for future research in this field and in treating renal diseases.

Declaration of interest. The authors have not reported any conflict of interest. The authors alone are responsible for the content and writing of the paper.

Acknowledgement. This study was supported by the Research Fund of Mersin University in Turkey (Project No. 2016-2-AP2-1811). This academic work was also supported by the TTO academic writing center of Mersin University.

REFERENCES

1. O. W. Moe. *Lancet*, **367**, 333–344 (2006).
2. F. L. Coe, A. Evan, E. Worcester, *J. Clin. Invest*., **115**, 2598–2608 (2005).
3. B. Y. Sun, Y. H. Lee, B. P. Jiaan, K. K. Chen, L. S. Chang, K. T. Chen, *J. Urol*., **156**, 903–905 (1996).
4. C. Türk, T. Knoll, A. Petrik, K. Sarica, A. Skolarikos, M. Straub, C. Seitz, *European Association of Urology*, 2015 guidelines.
5. N. L. Miller, A. P. Evan, J. E. Lingeman, *Urol. Clin. N. Am*., **34**, 295–313 (2007).
6. G. C. Curhan, *Urol. Clin. N. Am*., **34**, 287–293 (2007).
7. S. K. H. Khalil, A. Mohamad, *J. Appl. Sci. Res*., **3**, 387–391 (2007).
8. F. S. Manciu, J. R. Govani, W. G. Durrer, L. Reza, L. A. Pinales, *J. Raman Spectrosc*., **40**, 861–865 (2009).
9. E. N. Taylor, G. C. Curhan, *Kidney Int*., **70**, 835–839 (2006).
10. G. C. Curham, in: *Epidemiology/Urinary Tract Stone Disease*, Eds. P. N. Rao, G. M. Preminger, J. P. Kavanagh, Springer-Verlag, London, Part I, Chapter 1, 3–8 (2011).
11. E. K. Girija, S. N. Kalkaru, P. B. Sivaraman, Y. Yokogawa, *J. Sci. Ind. Res*., **66**, 632–639 (2007).
12. P. A. Bhat, P. Paul, *J. Chem. Sci*., **120**, 267–273 (2008).
13. G. Sahubert, *Urol. Res*., **34**, 146–150 (2006).
14. G. Sahubert, in: *Epidemiology/Urinary Tract Stone Disease*, Eds. P. N. Rao, G. M. Preminger, J. P. Kavanagh, Springer-Verlag, London, Part I, Chapter 29, 341–354 (2011).
15. F. L. Coe, J. H. Parks, J. R. Asplin, *N. Engl. J. Med*., **327**, 1141–1152 (1992).
16. K. Karthikeyan, K. Nanthakumar, P. Velmurugan, S. Tamilarasi, P. Lakshmana. *Environ. Monit. Assess*., **160**, 141–155 (2010).
17. R. Gilad, J. C. Williams Jr., K. D. Usman, R. Holland, S. Golan, R. Tor, D. Lifshitz, *J. Nephrol*., **30**, 135–140 (2017).
18. I. Singh. *Int. Urol. Nephrol*., **40**, 595–602 (2008).
19. G. Kanchana, P. Sundaramoorthi, G. P. Jeyanthi, *JMMCE*, **8**, 161–170 (2009).
20. V. Uvarov, I. Popov, N. Shapur, T. Abdin, O. N. Gofrit, D. Pode, M. Duvdevani, *Environ. Geochem. Health*, **33**, 613–622 (2011).
21. M. Kocademir, A. Baykal, M. Kumru, M. L. Tahmaz, *Spectrochim. Acta A*, **160**, 1–7 (2016).
22. A. A. Shemena, K. T. Arul, R. S Kumar, S. N. Kalkura, *Spectrochim. Acta A*, **134**, 442–448 (2015).
23. C. M. Corns, *Ann. Clin. Biochem*., **20**, 20–25 (1983).
24. I. A. Abboud, *Environ. Geochem. Health*, **30**, 445–463 (2008).
25. I. Dursun, H. M. Poyrazoglu, R. Dusunsel, Z. Gunduz, M. K. Gurgoze, D. Demirci, M. Kucukaydın, *Int. J. Nephrol. Urol*., **40**, 3–9 (2008).
26. A. Trinchieri, F. Rovera, R. Nespoli, A. Curro, *Arch. Ital. Urol., Androl.*, **64**, 251–262 (1996).
27. R. Chandrajith, G. Wijewardana, C. B. Dissanayake, A. Abeygunasekara, *Environ. Geochem. Health*, **28**, 393–399 (2006).
28. A. A. Al-Eisa, A. Al-Hunayyan, R. Gupta, *Int. Urol. Nephrol*., **33**, 3–6 (2002).
29. A. Kerr, M. Laing, *Environ. Geochem. Health*, **14**, 19–25 (1992).
30. A. Basiri, N. Shakhssalim, *Int. Urol. Nephrol*., **42**, 119–126 (2010).
31. A. Zarasvandi, E. J. M. Carranza, M. Heidari, E. Mousapour, *J. Afr. Earth. Sci*., **97**, 368–376 (2014).
32. R. S. Sai, B. Ranjit, K. M. Ganesh, G. Nageswara Rao, C. Janardhana, *Curr. Sci*., **94**, 104–109 (2008).
33. R. Selvaraju, A. Raja, G. Thiruppathi, *Spectrochim. Acta A*, **137**, 1397–1402 (2015).
34. A. H. Afaj, M. A. Sultan, *Sci. World J*., **5**, 24–38 (2005).
35. J. C. Williams Jr., E. Worcester, J. E. Lingeman, *Urolithiasis*, **45**, 19–25 (2017).
36. N. Vordos, S. Giannakopoulos, D. A. Gkika, J. W. Nolan, Ch. Kalaitzis, D. V. Bandekas, C. Kontogoulidou, A. Ch. Mitropoulos, S. Touloupidis, *Biochim. Biophys. Acta*, **1861**, No. 6, 1521–1529 (2017).
37. S. R. Barnela, S. S. Soni, S. S Saboo, A. S. Bhansali, *Indian J. Endocrinol. Metab*., **16**, No. 2, 236–239 (2012).
38. *Eating, Diet, & Nutrition for Kidney Stones*; https://www.niddk.nih.gov/health-information/urologic-diseases/kidney-stones/eating-diet-nutrition. Accessed: 28-Dec-2017.